Semarak International Journal of Nanotechnology

Journal homepage:
https://semarakilmu.com.my/journals/index.php/sijn/index

Porosity and Slip Velocity Effects on MHD Pulsatile Casson Fluid in a Cylinder

Wan Faezah Wan Azmi[1], Ahmad Qushairi Mohamad[1,*], Lim Yeou Jiann[1], Sharidan Shafie[1]

[1] Department of Mathematical Sciences, Faculty of Science, Universiti Teknologi Malaysia, 81310 UTM Johor Bahru, Johor, Malaysia

ARTICLE INFO

Article history:
Received : 15 March 2024
Received in revised form : 1 April 2024
Accepted : 28 April 2024
Available online : 10 June 2024

Keywords:
Blood Casson fluid; pulsatile flow; slip velocity; porous medium; MHD

ABSTRACT

Numerous researchers have extensively numerically investigated Casson fluid flow in a slip cylinder, resembling blood flow in human arteries. However, no study has successfully derived an analytical solution to validate the accuracy of the complex mathematical models obtained through numerical methods. This study focuses on utilizing Casson fluid to model blood flow in arteries with diameters ranging from 130 to 1300μm by analytical approach. The considered slip velocity is significant, closely mimicking challenges in real-world blood flow applications. Additionally, this research addresses the influence of magnetohydrodynamics (MHD), a porous medium simulating cholesterol plaque, and pulsatile pressure gradients simulating the rhythmic contraction of the heart. The problem is tackled using dual methods, incorporating Laplace and finite Hankel transform techniques. These techniques leverage versatile integral transformations to analytically resolve boundary value problems associated with time and cylindrical domains. The noteworthy outcomes emphasize that blood flow escalates with increasing slip velocity and pulsatile pressure gradient. This phenomenon is attributed to the increased velocity gradient between blood particles and the solid boundary as slip velocity rises. Furthermore, an elevated pressure gradient in blood flow leads to an increased force within blood vessels, directly accelerating blood flow. These findings are essential for addressing mathematical challenges related to blood diseases.

1. Introduction

The fluid consists of liquids and gases that can be deformed with the externally applied force and have no fixed shape. Fluid rheology can be broadly classified into two primary groups: Newtonian and non-Newtonian fluids. Non-Newtonian fluids, by definition, are against Newton's Law of Viscosity. In other words, it encompasses yield stress between shear stress and strain or has a nonlinear relationship. Since their features are multiplex and are indescribable by the conventional Navier-Stokes equations, they play a vital role in industrial and technological applications. Its applications are in polymer industries, oil and gas industries, biological systems, textiles, food technologies, and others. Its models have been presented in the literature. One of the best-known

* *Corresponding author.*
E-mail address: ahmadqushairi@utm.my

non-Newtonian liquids falls under the shear-thinning with yield stress category, which is Casson fluid [1]. It acts as an elastic solid when the yield stress is higher, but as soon as the external shear stress begins to dominate the yield stress, it begins to move or deform. This versatile fluid manifests in various everyday substances such as blood, tomato sauce, concentrated fruit juices, artificial fibres, honey, soup, and jelly [2]. Its distinctive properties have sparked significant interest among researchers, particularly in biomedical applications.

Besides that, investigating the fluid flow on heat transfer attracted many researchers, especially in free convection flow. Free convection or natural convection flow encompasses the motion of fluid masses, buoyancy, and gravitational forces, all influenced by temperature variations within the fluid flow. In summary, fluid movement arises from variations in density within a fluid caused by temperature gradients. It has numerous applications, such as in the biological industries, to diagnose diseases related to blood circulation, optimise foodstuff processing, oil industries, and others [3]. With such motivation, many researchers are interested in studying various geometries and fluids deeper. Ali *et al*., [4] conducted a heat transfer analytical investigation on the natural convection of Casson fluid flow over an oscillating plate. After that, Sheikh *et al*., [5] incorporate the chemical reactions effect on an oscillating plate into a similar problem as [4]. Khan *et al*., [6] and Mohamad *et al*., [7] researched Casson fluid flow between vertical channels with free convection. Aghighi *et al*., [8] discovered the Casson fluid flow's behaviour in a square enclosure with a free convection effect. An analytical model for Newtonian fluid was developed by Khan *et al*., [9] and Ahmed *et al*., [10], exploring the heat transfer phenomena generated by natural convection within a vertically oscillating cylinder. By employing a second-grade fluid, Javaid *et al*., [11] further explored the natural convection flow impact within a cylinder undergoing oscillations. Later, Jha *et al*., [12] conducted a study involving Newtonian fluid flow, where the investigation considered aspects such as free convection, heat sink/source, and chemical reactions. All the issues above were solved by using analytical and semi-analytical methods.

The magnetohydrodynamics (MHD) effect is among the contributing factors to heat transfer in free convection flow. Due to its manageable heat transfer rate, researchers' interest in MHD fluid flow has lately increased. External MHD causes Lorentz drag force to operate on the fluid, which opens the door to the potential of changing the fluid flow features on profiles for velocity and temperature [13]. Das *et al*., [14] explored and delved into the influences of magnetohydrodynamics (MHD) on the fluid rate and the heat transfer of Casson fluid as it flowed past a vertically oscillating plate. Sheikh *et al*., [15] evaluated the MHD flow effect for the Casson fluid model passed through a channel. The previously mentioned problems have all been analytically resolved via the Laplace transform method. Sanyal *et al*., [16] designed a model to explore the mathematical characteristics of blood in an inclined pulsatile flow with MHD and the effects of body acceleration. Mirza *et al*., [17] observed how the velocity effect influenced the second-grade MHD fluid flow in the cylinder. Ali *et al.*, [18]–[22] aimed to understand the MHD and the heat transfer effect on Casson fluid flow past the cylinder. Containing various fluid model types, investigations are being conducted into how the MHD impacts pulsatile Blood flow in a magnetic particle-filled cylindrical tube [23]–[25]. All researchers could obtain analytical solutions by applying the Laplace and Hankel transformation. However, none of them solves the problems of MHD flow in a porous medium.

Petroleum, textiles, polymers, biological systems, and irrigation issues are a few areas where the MHD flow in a porous media has applications [26]. Particularly in biological applications to track the impact of cancer cell treatment with temperature fluctuations in living tissue, there is a crucial requirement for fluid movement via porous media [27]. Kataria *et al*., [28]–[30] and Iftikhar *et al*., [31] also explored the MHD Casson fluid flow effect through a porous material atop an accelerating and oscillating vertical plate, considering the diverse heat and mass transfer influences. Many

scholars have looked at the issues with MHD flow inside a cylindrical region of a porous media in recent years. A mathematical model was devised by Rathod and Tanveer [32] to consider the impact of MHD and body acceleration on the pulsatile flow of blood through a rigid tube. The Newtonian fluid flow's analytical solution within a moving porous cylinder was obtained by Paul [33], considering the influences of MHD and free convection. The porosity and MHD effects on the Newtonian fluid's pulsating flow have been investigated by Bansi *et al*., [34] and Abro and Atangana [35]. Maiti *et al.,* [36], [37] extended a similar problem as previous study [35] by using the Casson fluid model with the additional thermal radiation effect. As mentioned above, they obtained analytical solutions to the MHD and porosity effects problem of fluid flow.

All the previous studies above discussed no-slip boundary conditions. Despite this, the slip velocity at the boundary has advantages in several scenarios, including applications like the oil and gas sector for the drilling process and the blood circulation in human arteries. The idea that slip velocity at a wall is in close connection to the shear stress at the border was first put out by Navier in 1823 [38]. Slip is the fluid's finite velocity observed at or near a boundary [39]. Inspired by his work, numerous scholars have conducted numerical investigations to explore issues related to Casson fluid flow in a cylindrical domain, accounting for the slip effect at the boundary. Exploring the effects of slip velocity on Casson fluid flow within a cylindrical domain in the presence of the MHD effect, Ahmed and Hazarika [40] stand as early contributors. They tackled the problem numerically, utilizing the shooting method. Murthy *et al.*, [41] investigated the momentum and energy equations associated with Casson fluid flow around a stretching cylinder, incorporating slip velocity and MHD effects into their analysis. They utilized numerical techniques, specifically the Runge-Kutta method, to solve the problem. Studying the impact of slip on Casson fluid flow in a porous medium outside a stretching cylinder, Ullah *et al.*, [42] investigated the effects of MHD, thermal radiation, viscous dissipation, and Joule heating. The researchers employed the Keller box method to address this problem. Next, Jalil and Iqbal [43] conducted a numerical investigation on Casson fluid flow over an exponentially stretching cylinder, considering the effects of suction and blowing. They omitted the energy equation from the momentum equation and solved the system using the Keller box method. Hayat *et al.*,[44] employed the Homotopy Analysis Method (HAM) to derive a semi-analytical solution for the Casson fluid flow in a slip cylinder. The effects of heat and mass transfer were evaluated. All of the studies mentioned above have generated numerical and semi-analytical solutions for Casson fluid flow through a cylinder, taking into consideration slip effects at the boundary.

As far as the authors are aware, numerous researchers have numerically explored Casson fluid flow with slip boundary effects in cylinders. However, prior literature lacks analytical solutions for Casson fluid flow in a slipping vertical cylinder, incorporating the influences of MHD, porous medium, and heat transfer. Hence, the objective of this current investigation is to examine the Casson fluid's unsteady free convection movement via a porous medium (simulating cholesterol plaque) and a vertical cylinder while considering the impacts of slip velocity, MHD, and pulsatile pressure gradient (simulating the rhythmic contraction of the heart). Analytical solutions for fluid velocity and temperature within the cylindrical domain were obtained using Laplace and finite Hankel transform methods. Maple software was utilized to compute several essential parameters, and Bessel functions of zero order were employed to depict the graphical solutions.

2. Problem Formulation

An incompressible Casson fluid with free convection flow is considered within the framework of a vertical cylinder with a radius of r_0. The r is the radial coordinate, which is oriented perpendicular to the vertically oriented z-axis. The pulsatile pressure gradient is one of the factors induced by fluid

flow. The porous medium and the external magnetic field both had an impact. The external electric field, the resulting magnetic field, and the electric field induced by polarisation all have negligible significance. The fluid and the cylinder are idle during t^*=0, and the temperature is ambient, T_∞. The fluid begins its flow with a slip velocity at the cylinder wall surface after the initial time t^*>0. Inside the cylinder, the temperature gradually increases from the initial ambient temperature, T_∞, to reach the wall temperature, T_w, and is then held at a constant level. The fluid velocity and fluid temperature solely depend on the variables *r* and *t*. The problem of fluid flow is visually represented in the physical diagram in Figure 1.

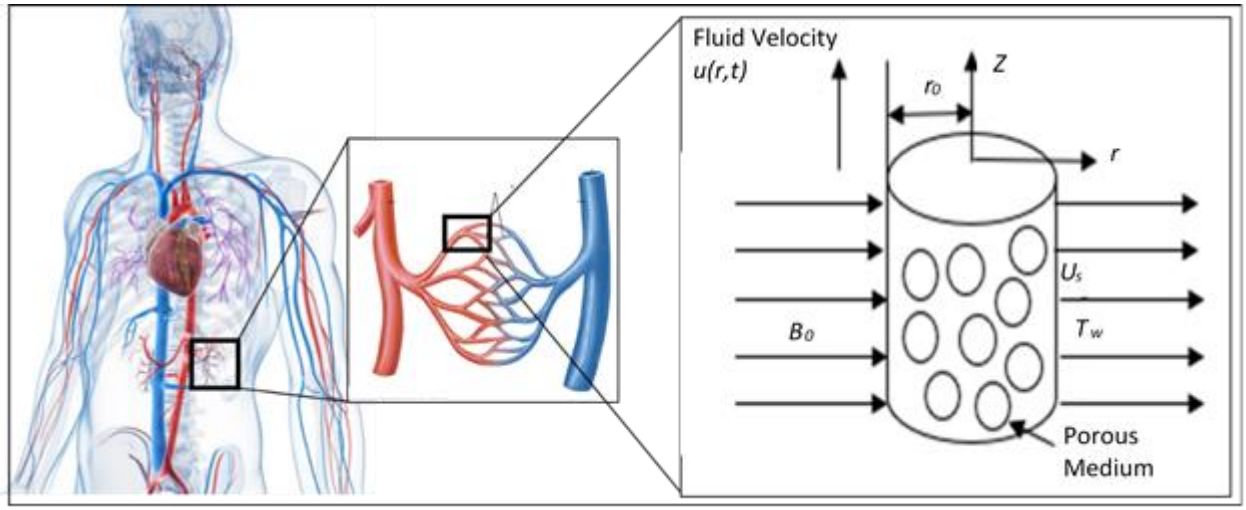

Fig. 1. The fluid flow physical geometry [45]

Describing the relation between shear stress and strain rate in the context of incompressible Casson fluid flow, the equation is as follows [37]

$$\tau_{ij} = \begin{cases} 2\left(\mu_B + \dfrac{p_y}{\sqrt{2\pi}}\right)e_{ij}; & \pi > \pi_c \\ 2\left(\mu_B + \dfrac{p_y}{\sqrt{2\pi_c}}\right)e_{ij}; & \pi < \pi_c \end{cases} \tag{1}$$

where π is the deformation rate component product representing $e_{ij}e_{ij}$ with e_{ij} denoting the (*i*,*j*)-th component of the deformation rate. π_c is a critical value of this product according to the non-Newtonian model. Additionally, μ_B stands for the plastic dynamic viscosity of non-Newtonian fluid, and p_y denotes the yield stress of fluid. The continuity equation is automatically fulfilled built on the provided assumptions, Boussinesq's approximation, and the neglect of viscous dissipation. As a result, the equation for momentum and energy governs the problem as the governing equations [19], [37]

$$\rho\frac{\partial u^*}{\partial t^*} = -\frac{\partial p^*}{\partial z^*} + \mu\left(1+\frac{1}{\beta}\right)\left(\frac{\partial^2 u^*}{\partial r^{*2}} + \frac{1}{r^*}\frac{\partial u^*}{\partial r^*}\right) - \frac{\mu}{k_p}u^* - \sigma B_0^2 u^* + g\rho\beta_T\left(T^* - T_\infty\right) \tag{2}$$

$$\rho c_p \frac{\partial T^*}{\partial t^*} = k\left(\frac{\partial^2 T^*}{\partial r^{*2}} + \frac{1}{r^*}\frac{\partial T^*}{\partial r^*}\right) \tag{3}$$

accompanied by the proper initial and boundary conditions [19], [46]

$$\begin{aligned} &u^*(r^*,0)=0 \qquad T^*\left(r^*,0\right)=T_\infty \qquad ;\ r\in[0,r_0], \\ &u^*(r_0^*,t^*)=u_s^* \qquad T^*\left(r_0^*,t^*\right)=T_w \qquad ;\ t^*>0 \end{aligned} \tag{4}$$

where ρ is the fluid's density, the velocity component along the z-axis u^*, the pressure gradient p, fluid dynamic viscosity μ, the non-Newtonian Casson parameter $\beta=\mu_B\sqrt{2\pi_c}/\tau_y$, permeability constant k_p, electrical conductivity σ, applied magnetic field strength B_0, the gravitational acceleration g, the thermal expansion coefficient β_T, the fluid temperature T^*, the specific heat capacity of fluid c_p, the thermal conductivity k, the fluid kinematic viscosity v. Introducing dimensionless variables in a manner suitable for the context [17], [19], [46]

$$t=\frac{t^*\nu}{r_0^2}, r=\frac{r^*}{r_0}, u=\frac{u^*}{u_0}, u_s=\frac{u_s^*}{u_0}, z=\frac{z^*}{r_0}, p=\frac{p^* r_0}{\mu u_0}, \theta=\frac{T-T_\infty}{T_w-T_\infty}. \tag{5}$$

Substituting the dimensionless variables (5) into Eqs. (2), (3), and (4) produces the momentum and energy equations outlined below

$$\frac{\partial u}{\partial t} = -\frac{\partial p}{\partial z} + \beta_1\left(\frac{\partial^2 u}{\partial r^2} + \frac{1}{r}\frac{\partial u}{\partial r}\right) - \frac{1}{Da}u - Mu + Gr\theta, \tag{6}$$

$$\frac{\partial \theta}{\partial t} = \frac{1}{\Pr}\left(\frac{\partial^2 \theta}{\partial r^2} + \frac{1}{r}\frac{\partial \theta}{\partial r}\right) \tag{7}$$

Accompanied by the correlated dimensionless initial and boundary conditions

$$\begin{aligned} &u(r,0)=0, \qquad \theta\left(r,0\right)=0 \qquad ;\ r\in[0,1]\ , \\ &u(1,t)=u_s, \qquad \theta\left(1,t\right)=1 \qquad ;\ t>0 \end{aligned} \tag{8}$$

where $Da=\frac{k_p}{r_0^2}$ denotes the Darcy number, $M=\frac{\sigma B_0^2 r_0^2}{\rho\nu}$ signifies the magnetic parameter, $\Pr=\frac{\mu c_p}{k}$ is the Prandtl number, $Gr=\frac{g\beta_T\left(T_w-T_\infty\right)r_0^2}{\nu u_0}$ represents the Grashof number, $\beta_1=\frac{1}{\beta_0}$ and $\beta_0=1+\frac{1}{\beta}$ are the constant parameters. The pulsatile pressure gradient arises from the rhythmic pumping motion of the heart, as explained [37]

$$-\frac{\partial p}{\partial z} = A_0 + A_1\cos\left(\omega t\right) \tag{9}$$

where A_0 and A_1 are the amplitude of pulsatile flow, ω defined as the frequency of pulsatile flow. Substitutes Eq. (9) into Eq. (6), which yields

$$\frac{\partial u}{\partial t} = \left(A_0 + A_1 \cos\left(\omega t\right)\right) + \beta_1 \left(\frac{\partial^2 u}{\partial r^2} + \frac{1}{r}\frac{\partial u}{\partial r}\right) - \frac{1}{Da}u - Mu + Gr\theta. \tag{10}$$

3. Problem Solution

In the subsequent phase, a dual approach is employed, combining the Laplace transform and finite Hankel transform. This methodology is applied for the analytical solution of the dimensionless partial differential equations and their corresponding initial and boundary conditions.

3.1 Temperature Profile

Laplace transform is being utilised in energy equation (7) and initial and boundary conditions (8), which yields

$$s\bar{\theta}(r,s) = \frac{1}{\Pr}\left[\frac{d^2\bar{\theta}(r,s)}{dr^2} + \frac{1}{r}\frac{d\bar{\theta}(r,s)}{dr}\right], \tag{11}$$

$$\bar{\theta}(1,s) = \frac{1}{s} \tag{12}$$

where $\bar{\theta}(r,s)$ represents the function for Laplace transform $\theta(r,t)$ and s refer to the transformation variable. Subsequently, utilising the zero-order finite Hankel transform to Eq. (11) under condition (12) yields the following result

$$\overline{\theta_H}(r_n,s) = \frac{J_1\left(r_n\right)}{r_n}\left[\frac{1}{s} - \frac{1}{s + \frac{r_n^2}{\Pr}}\right] \tag{13}$$

where the finite Hankel transform of the function $\bar{\theta}(r,s)$ is defined as $\bar{\theta}_H(r_n,s) = \int_0^1 r\bar{\theta}(r,s)J_0\left(rr_n\right)dr$ and the positive roots r_n with n=0,1,… determined by the equation $J_0(x) = 0$, where J_0 represents the zero-order first-kind Bessel function, and J_1 is the first-order Bessel function of the first kind. Next, the equation below is result in exploiting the inverse Laplace transform on Eq. (13)

$$\theta_H(r_n,t) = \frac{J_1\left(r_n\right)}{r_n}\left(1 - \exp\left(-\frac{r_n^2}{\Pr}t\right)\right). \tag{14}$$

Concludingly, the order zero for inverse finite Hankel transform can be impressed as follows

$$H_0^{-1}\theta_H\left(r_n,t\right)=\theta\left(r,t\right)=2\sum_{n=1}^{\infty}\frac{J_0\left(rr_n\right)}{J_1^2\left(r_n\right)}\theta_H\left(r_n,t\right), \tag{15}$$

and applying to Eq. (14) and the analytical solution for the energy equation for the pulsatile Casson fluid flow is

$$\theta(r,t)=1-2\sum_{n=1}^{\infty}\frac{J_0\left(rr_n\right)}{r_nJ_1\left(r_n\right)}\exp\left(-\frac{r_n^2}{\mathrm{Pr}}t\right). \tag{16}$$

3.2 Velocity Profile

The Laplace transform had been utilised on both the momentum equation (Eq. 10) and the boundary condition (Eq. 8), all while taking into account the initial state (Eq. 8). This process results in the following outcome

$$s\bar{u}(r,s)=\frac{A_0}{s}+\frac{A_1s}{s^2+\omega^2}+\beta_1\left[\frac{d^2\bar{u}(r,s)}{dr^2}+\frac{1}{r}\frac{d\bar{u}(r,s)}{dr}\right]-\frac{1}{Da}\bar{u}(r,s)-M\bar{u}(r,s)+Gr\bar{\theta}\left(r,s\right), \tag{17}$$

$$\bar{u}(1,s)=\frac{u_s}{s}. \tag{18}$$

Introducing the notation $\bar{u}(r,s)$ to signify the Laplace transform of the function $u(r,t)$. Afterwards, we utilise a zero-order finite Hankel transform to Eq. (17) while incorporating boundary condition (18), resulting in

$$\bar{u}_H(r_n,s)=\left[\frac{A_0}{s}+\frac{A_1s}{s^2+\omega^2}+\beta_1r_n^2\frac{u_s}{s}+Gr\left(\frac{1}{s}-\frac{1}{s+\frac{r_n^2}{\mathrm{Pr}}}\right)\right]\frac{J_1\left(r_n\right)}{r_n}\frac{1}{s+c_1} \tag{19}$$

where $c_1=\frac{1}{Da}+M+\beta_1r_n^2$ and $\bar{u}_H(r_n,s)=\int_0^1 r\bar{u}(r,s)J_0\left(rr_n\right)dr$ is the finite Hankel transform of the function $\bar{u}(r,s)$. Employing inverse Laplace transform on Eq. (19)

$$u_H\left(r_n,t\right)=\frac{J_1\left(r_n\right)}{r_n}\left[u_{H1}\left(r_n,t\right)+u_{H2}\left(r_n,t\right)+u_{H3}\left(r_n,t\right)+u_{H4}\left(r_n,t\right)-u_{H5}\left(r_n,t\right)\right] \tag{20}$$

With

$$u_{H1}\left(r_n,t\right)=\frac{A_0}{c_1}\left(1-\exp\left(-c_1t\right)\right), \tag{21}$$

$$u_{H2}\left(r_n,t\right)=\frac{A_1}{c_1^2+\omega^2}\left(\omega\sin\left(\omega t\right)+c_1\left(\cos\left(\omega t\right)-\exp\left(-c_1t\right)\right)\right), \tag{22}$$

$$u_{H3}\left(r_n,t\right)=u_s\left(1-\exp\left(-c_1t\right)-\frac{c_2\left(1-\exp\left(-c_1t\right)\right)}{c_2+\beta_1r_n^2}\right), \tag{23}$$

$$u_{H4}\left(r_n,t\right)=\frac{Gr}{c_1}\left(1-\exp\left(-c_1t\right)\right), \tag{24}$$

$$u_{H5}\left(r_n,t\right)=\frac{Gr\,\mathrm{Pr}}{\mathrm{Pr}\,c_1-r_n^2}\left(\exp\left(-\frac{r_n^2}{\mathrm{Pr}}t\right)-\exp\left(-c_1t\right)\right) \tag{25}$$

where $c_2=\frac{1}{Da}+M$ is a constant parameter. The given result is the zero-order inverse finite Hankel transform

$$H_0^{-1}u_H\left(r_n,t\right)=u\left(r,t\right)=2\sum_{n=1}^{\infty}\frac{J_0\left(rr_n\right)}{J_1^2\left(r_n\right)}u_H\left(r_n,t\right), \tag{26}$$

being applied to Eq. (20), and the analytical solution for the momentum equation for pulsatile Casson fluid flow is as below

$$u\left(r,t\right)=u_s+2\sum_{n=1}^{\infty}\frac{J_0\left(rr_n\right)}{r_nJ_1\left(r_n\right)}\left[-v_1\left(r,t\right)+v_2\left(r,t\right)+v_3\left(r,t\right)\right] \tag{27}$$

With

$$v_1\left(r,t\right)=u_s\left(\exp\left(-c_1t\right)+\frac{c_2\left(1-\exp\left(-c_1t\right)\right)}{c_2+\beta_1r_n^2}\right), \tag{28}$$

$$v_2\left(r,t\right)=\frac{A_0}{c_1}\left(1-\exp\left(-c_1t\right)\right)+\frac{A_1}{c_1^2+\omega^2}\left(\omega\sin\left(\omega t\right)+c_1\left(\cos\left(\omega t\right)-\exp\left(-c_1t\right)\right)\right), \tag{29}$$

$$v_3\left(r,t\right)=Gr\left(\frac{1-\exp\left(-c_1t\right)}{c_1}-\frac{\mathrm{Pr}}{\mathrm{Pr}\,c_1-r_n^2}\left(\exp\left(\frac{-r_n^2}{\mathrm{Pr}}t\right)-\exp\left(-c_1t\right)\right)\right). \tag{30}$$

4. Results and Discussions

The Maple software is solving analytical for fluid velocity $u(r,t)$ and temperature $\theta(r,t)$ profiles to determine the flow behaviour. It is calculated and graphically displays the slip influence on the temperature and velocity of the fluid. Figures 2-4 show the several dimensionless effects parameters,

which are Casson parameter β, Grashof number *Gr*, Prandtl number Pr, Darcy number *Da*, Magnetic parameter *M*, amplitude pulsatile pressure gradient A_0, A_1, and time parameter *t*.

These parametric values are kept constant for numerical calculations: A_0=0.05, A_1=0.05, $\omega=\pi/4$, β=0.8, *Da*=1, *M*=1, *Gr*=1, *t*=1 [7], [36], [46]. Pr=21 is chosen since the current study involves human blood flow. These results in Eq. (27) will be contrasted with the findings documented in earlier publications for accuracy verification, completed by Khan *et al*., [9], as shown in Figure 2. The recent research focused on the convective and Casson fluid for pulsatile flow. The effects of MHD, porosity, and slip velocity are also considered in this study. Khan *et al*., [9] investigated the Newtonian fluid flows convectively past an oscillating cylinder. For comparison, some parameters have been set as A_0=0, A_1=0, ω=0, $\beta=\infty$, $Da=\infty$, *M*=0, and u_s=1 to obtain the same formation for both problems.

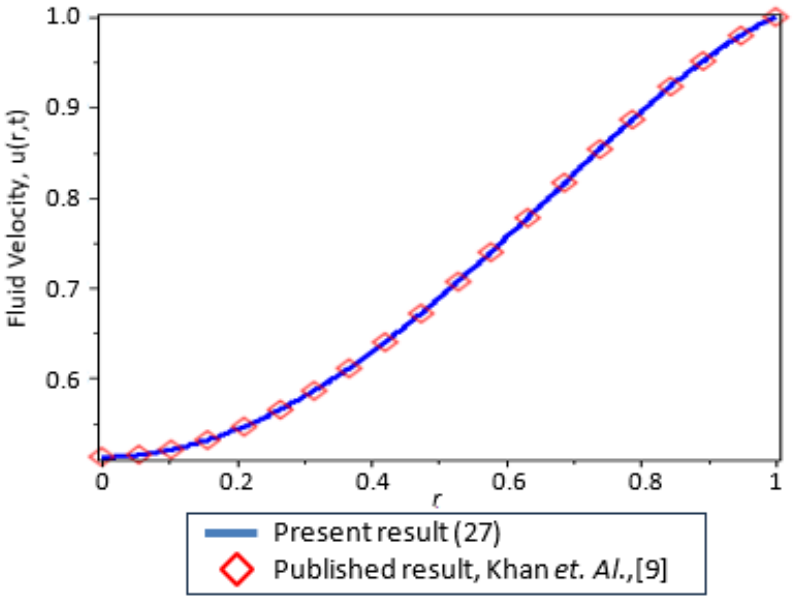

Fig. 2. Present result validation of fluid velocity *u*(r,*t*)

In Figure 3, how blood velocity distributions are affected by variations in the Casson parameter (β) in the slip velocity presence and its absence is being visualised. The Casson fluid behaviour becomes more effective when the Casson parameter is close to zero, which is relevant to the blood flow properties in capillaries. In scenarios where the Casson parameter exhibits high values ($\beta\rightarrow\infty$), the current fluid model behaves like a Newtonian fluid. According to the graph, blood flow decreases with higher Casson parameter values when a no-slip condition occurs. This decrease is attributed to the rise in plastic dynamic viscosity, leading to increased internal friction force and, subsequently, a higher shear thickening factor, making the blood more viscous.

Conversely, blood flow increases with higher Casson parameter values in the presence of slip effect. It is associated with a decrease in the yield stress of the blood, which reduces the force required to initiate blood flow, thus accelerating blood flow velocity. Eventually, both slip and no-slip cases reach an equilibrium state where blood flow at both the wall and centre exhibit similar behaviour, showing a decline due to the increased Casson parameter and blood viscosity. Hence, the Casson parameter's impact on blood flow is significant in medical contexts, as it can influence the hemodynamics of blood flow in narrow arteries.

Figure 4 illustrates blood flow profiles corresponding to varying Darcy number, *Da*. The observation reveals that blood flow increases as the Darcy number increases, indicating changes in the porous medium conditions. Physically, a higher Darcy number suggests more excellent

permeability within the porous medium. Permeability refers to the medium's ability to facilitate fluid movement [1]. In other words, as permeability increases, the porous medium becomes more effective in transmitting blood particles, potentially leading to reduced formation of fatty plaque in the blood vessel. Consequently, this enhancement in permeability augments blood flow velocity under both slip and no-slip conditions.

The magnetic parameter, *M*, depicted in Figure 5, plays a pivotal role in shaping blood velocity profiles. As the magnetic parameter increases, there is a concurrent decrease in blood flow velocity, regardless of whether non-slip or slip velocities are observed at the cylinder wall. This phenomenon is attributed to the emergence of the Lorentz force, which acts as a resistance against fluid movement. The Lorentz force arises from the interaction between induced currents and the magnetic field, opposing blood flow within the arteries. The presence of an external magnetic field induces currents in the flowing blood, contributing to this resistance. Consequently, the magnetic field's influence significantly modulates blood circulation within the human vascular system [47].

Figure 6 portrays the effect of the thermal Grashof number on blood flow profiles, illustrating scenarios with both slip and no-slip conditions at the boundary. The Grashof number, which denotes the ratio between thermal buoyancy force and hydrodynamic forces, is highlighted [29]. As the thermal Grashof number increases, blood velocity also rises, regardless of the presence or absence of slip velocity effects at the boundary conditions. The thermal buoyancy force, arising from variations in blood density and temperature gradients, becomes predominant during free convection. When blood temperature rises, its density decreases, resulting in reduced impact on the viscous force of blood. This leads to upward movement driven by buoyancy forces, while blood with higher density moves downward due to gravity forces. Consequently, there is an increase in blood velocity.

Figure 7 displays the impact of the pulsatile pressure gradient on blood flow profiles, considering slip and no-slip conditions. The pulsatile pressure gradient serves as an indicator of the cardiac pumping mechanism, characterized by two parameters, which are a constant amplitude denoted as A_0 and an amplitude of oscillating velocity denoted as A_1. According to Hemmat Esfe *et al.,* [48], these parameters reflect the nature of blood flow in arteries. Analysis of the graph demonstrates that increasing the parameters of the pulsatile pressure gradient leads to an increase in blood flow under both slip and no-slip conditions. The amplification of pulsatile flow indicates strengthening of the cardiac pumping mechanism, facilitating accelerated blood flow throughout the human vascular system. The regulation of pulsatile pressure gradients holds the potential for mitigating or managing various conditions, including hypertension, which arises from blood flow obstruction.

In correlation to the Prandtl number, there are changes in the blood velocity and temperature, as revealed in Figures 8-9. The Prandtl number is defined as the reciprocal of the ratio of momentum to thermal diffusivity [14]. In the context of blood flow in arteries, the Prandtl number is significant in understanding the balance between momentum diffusion and thermal diffusion. The trend observed in Figure 8 indicates a decline in blood velocity with a rise in the Prandtl number, irrespective of slip velocity. A higher Prandtl number signifies increased blood viscosity, meaning viscous forces dominate over thermal forces. Consequently, the blood becomes thicker, and experiences increased frictional forces, resulting in slower motion.

However, the Prandtl number influences the blood temperature, $\theta(r,t)$ versus radial coordinate *r*, which has been reflected in Figure 9 for different time values, *t*. Blood temperature diminishes as the Prandtl number increases. This phenomenon occurs because a higher Prandtl number accelerates heat diffusion due to the inverse correlation between thermal diffusivity and the Prandtl number. Consequently, the diminished convective heat transfer rate results in a slower temperature change within the fluid, leading to a reduction in fluid temperature. Furthermore, with high time *t* values,

the Prandtl number substantially impacts the temperature distribution. Understanding the Prandtl number in blood flow is essential for evaluating the effectiveness of heat transfer mechanisms within the bloodstream, with implications for understanding heat exchange dynamics in physiological processes such as thermoregulation and the vascular response to temperature changes.

The impact of slip velocity on blood flow profiles is showcased in Figures 3-8. The graphs illustrate that the slip effect results in a reduction in blood flow velocity as it approaches the centre of the cylinder. This decline in velocity occurs due to increased viscous forces encountered by the blood as it moves toward the cylinder's centre. Additionally, velocity increases with higher slip velocities, particularly near the cylinder wall. This phenomenon arises from the minimal shear stress, resulting in a reduced velocity gradient near the boundary. Consequently, this leads to a decrease in blood viscosity and an increase in blood flow. Understanding the impact of slip velocity on blood flow in arteries is essential for precise modelling and prediction of hemodynamic behaviours, as well as for elucidating the physiological and pathological mechanisms underlying vascular function.

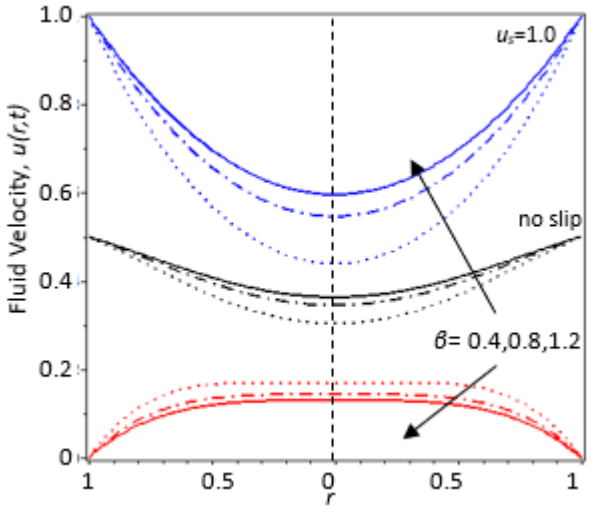

Fig. 3. Blood velocity and Casson Parameter *B* with slip and no-slip effect

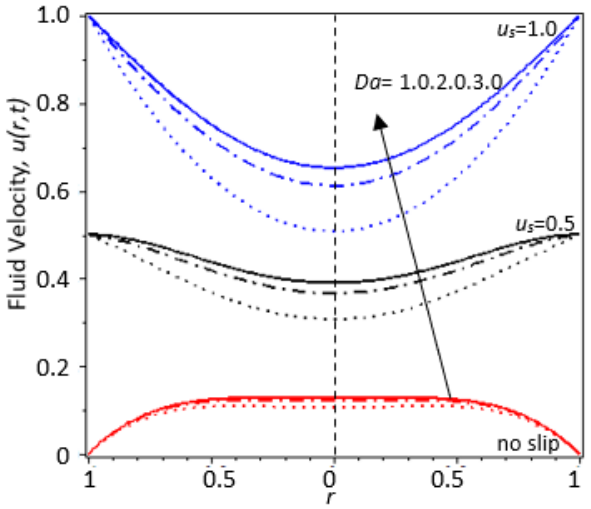

Fig. 4. Blood velocity and Darcy number *Da* with slip and no-slip effect

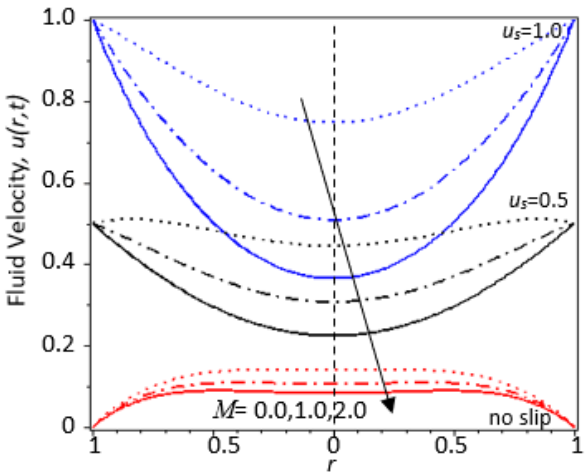

Fig. 5. Blood velocity and Magnetic parameter *M* with slip and no-slip effect

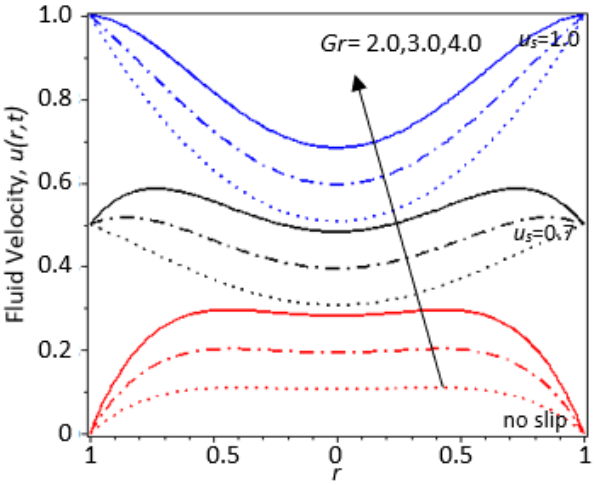

Fig. 6. Blood velocity Grashof number *Gr* with slip and no-slip effect

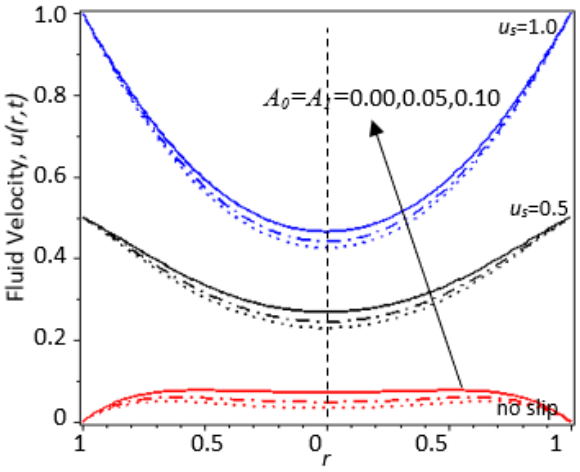

Fig. 7. Blood velocity and amplitude pulsatile pressure gradient A_0, A_1 with slip and no-slip effect

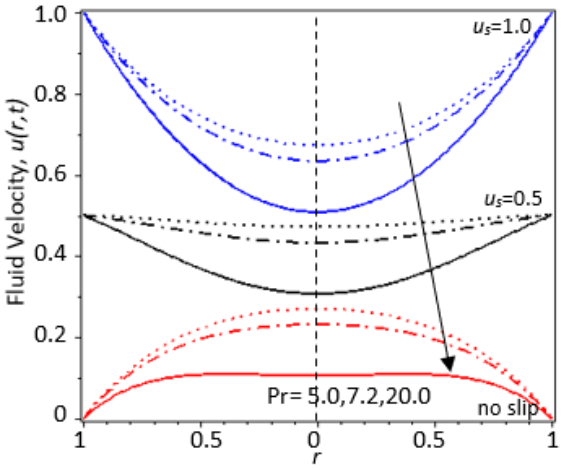

Fig. 8. Fluid velocity and Prandtl number Pr with slip and no-slip effect

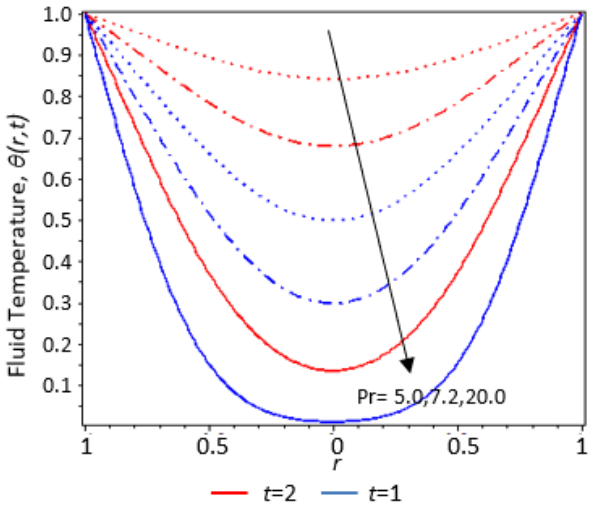

Fig. 9. Fluid temperature and Prandtl number Pr

5. Conclusions

This study investigates how the slip velocity presence at the boundary affects the unsteady MHD-free convection flow of blood Casson fluid in a porous medium within a vertical cylinder. These analytical solutions fulfil the corresponding initial and boundary conditions. Comparing the current findings to previously published findings from Khan *et al*., [9] and obtaining agreement for both comparisons constitutes result validation. The distribution of temperature and velocity varies due to the changes of the slip parameter u_s, Darcy number *Da*, Casson parameter β, Grashof number *Gr*, magnetic parameter *M*, amplitude pulsatile pressure gradient A_0, A_1, and Prandtl number Pr have been analysed. From this analysis, the results can be concluded as:

i. The blood velocity increases as u_s, *Gr*, *Da*, A_0, A_1, and *t* increase.
ii. The blood velocity declines when *M* and Pr increase.
iii. The augmentation of the Prandtl number and the time reduction resulted in a decline in temperature profiles.

iv. Slip velocity influences the behaviour of blood flow. When β increases, blood velocity rises for slip u_s while decreases for no-slip.

The results obtained from this study serve as important preliminary hypotheses for understanding and managing the processes of blood flow and heat transfer within the human body. These insights can be instrumental in analyzing blood circulation patterns during cancer treatments, facilitating drug delivery through the bloodstream, and addressing other pertinent medical scenarios. Additionally, this research presents opportunities for broader investigations into fluids containing nanoparticles, the effects of radiation exposure, and chemical reactions.

.

Acknowledgement
The authors received financial support for the research, authorship, and publication of this article from Universiti Teknologi Malaysia under Grant Scheme (R.J130000.7354.4B748) and Matching Grant Scheme (Q.J130000.3054.03M77).

References

[1] Sochi, Taha. "Non-Newtonian flow in porous media." *Polymer 51*, no. 22 (2010): 5007-5023. https://doi.org/10.1016/j.polymer.2010.07.047

[2] Anwar, Talha, Poom Kumam, and Wiboonsak Watthayu. "Unsteady MHD natural convection flow of Casson fluid incorporating thermal radiative flux and heat injection/suction mechanism under variable wall conditions." *Scientific Reports* 11, no. 1 (2021): 4275. https://doi.org/10.1038/s41598-021-83691-2

[3] Divya, B. B., G. Manjunatha, C. Rajashekhar, Hanumesh Vaidya, and K. V. Prasad. "Analysis of temperature dependent properties of a peristaltic MHD flow in a non-uniform channel: A Casson fluid model." *Ain Shams Engineering Journal* 12, no. 2 (2021): 2181-2191. https://doi.org/10.1016/j.asej.2020.11.010

[4] Ali, Farhad, Nadeem Ahmad Sheikh, Ilyas Khan, and Muhammad Saqib. "Solutions with Wright function for time fractional free convection flow of Casson fluid." *Arabian Journal for Science and Engineering* 42 (2017): 2565-2572. https://doi.org/10.1007/s13369-017-2521-3

[5] Sheikh, Nadeem Ahmad, Farhad Ali, Muhammad Saqib, Ilyas Khan, Syed Aftab Alam Jan, Ali Saleh Alshomrani, and Metib Said Alghamdi. "Comparison and analysis of the Atangana–Baleanu and Caputo–Fabrizio fractional derivatives for generalized Casson fluid model with heat generation and chemical reaction." *Results in physics* 7 (2017): 789-800. https://doi.org/10.1016/j.rinp.2017.01.025

[6] Khan, Ilyas, Muhammad Saqib, and Farhad Ali. "Application of time-fractional derivatives with non-singular kernel to the generalized convective flow of Casson fluid in a microchannel with constant walls temperature." *The European Physical Journal Special Topics* 226 (2017): 3791-3802. https://doi.org/10.1140/epjst/e2018-00097-5

[7] Qushairi, Mohamad Ahmad, Jiann Lim Yeou, Sharidan Shafie, Ilyas Khan, and Zulkhibri Ismail. "Exact solution for unsteady free convection flow of Casson fluid in vertical channel." In *MATEC Web of Conferences*, vol. 189, p. 01007. EDP Sciences, 2018. https://doi.org/10.1051/matecconf/201818901007

[8] Aghighi, Mohammad Saeid, Christel Metivier, and Hamed Masoumi. "Natural convection of Casson fluid in a square enclosure." *Multidiscipline Modeling in Materials and Structures* 16, no. 5 (2020): 1245-1259. https://doi.org/10.1108/MMMS-11-2019-0192

[9] Khan, Ilyas, Nehad Ali Shah, Asifa Tassaddiq, Norzieha Mustapha, and Seripah Awang Kechil. "Natural convection heat transfer in an oscillating vertical cylinder." *PloS one* 13, no. 1 (2018):

e0188656. https://doi.org/10.1371/journal.pone.0188656

[10] Ahmed, Najma, Nehad Ali Shah, and Dumitru Vieru. "Natural convection with damped thermal flux in a vertical circular cylinder." *Chinese journal of physics* 56, no. 2 (2018): 630-644. https://doi.org/10.1016/j.cjph.2018.02.007

[11] Javaid, Maria, M. Imran, M. A. Imran, I. Khan, and K. S. Nisar. "Natural convection flow of a second grade fluid in an infinite vertical cylinder." *Scientific Reports* 10, no. 1 (2020): 8327. https://doi.org/10.1038/s41598-020-64533-z

[12] Jha, Basant K., Sylvester B. Joseph, and Abiodun O. Ajibade. "Role of diffusion thermo on unsteady natural convection of a chemically reactive fluid impacted by heat source/sink in a tube." *Journal of Taibah University for Science* 16, no. 1 (2022): 495-504. https://doi.org/10.1080/16583655.2022.2078135

[13] Makkar, Vinita, Vikas Poply, Rangoli Goyal, and Naresh Sharma. "Numerical investigation of mhd casson nanofluid flow towards a non linear stretching sheet in presence of double-diffusive effects along with viscous and ohmic dissipation." *Journal of Thermal Engineering* 7, no. 2 (2021): 1-17. https://doi.org/10.18186/thermal.859221

[14] Das, M., R. Mahato, and R. Nandkeolyar. "Newtonian heating effect on unsteady hydromagnetic Casson fluid flow past a flat plate with heat and mass transfer." *Alexandria Engineering Journal* 54, no. 4 (2015): 871-879. https://doi.org/10.1016/j.aej.2015.07.007

[15] Sheikh, Nadeem Ahmad, Dennis Ling Chuan Ching, Thabet Abdeljawad, Ilyas Khan, Muhammad Jamil, and Kottakkaran Sooppy Nisar. "A fractal-fractional model for the MHD flow of Casson fluid in a channel." *Comput. Mater. Contin* 67, no. 2 (2021): 1385-1398. https://doi.org/10.32604/cmc.2021.011986

[16] Sanyal, D. C., K. Das, and S. Debnath. "Effect of magnetic field on pulsatile blood flow through an inclined circular tube with periodic body acceleration." (2007).

[17] Mirza, Itrat Abbas, Muhammad Saeed Akram, and Imran Siddique. "Flows of a generalized second grade fluid in a cylinder due to a velocity shock." *Chinese Journal of Physics* 60 (2019): 720-730. https://doi.org/10.1016/j.cjph.2019.06.009

[18] Ali, Farhad, Nadeem Ahmad Sheikh, Ilyas Khan, and Muhammad Saqib. "Magnetic field effect on blood flow of Casson fluid in axisymmetric cylindrical tube: A fractional model." *Journal of Magnetism and Magnetic Materials* 423 (2017): 327-336. https://doi.org/10.1016/j.jmmm.2016.09.125

[19] Ali, Farhad, Nabeel Khan, Anees Imtiaz, Ilyas Khan, and Nadeem Ahmad Sheikh. "The impact of magnetohydrodynamics and heat transfer on the unsteady flow of Casson fluid in an oscillating cylinder via integral transform: A Caputo–Fabrizio fractional model." *Pramana* 93, no. 3 (2019): 47. https://doi.org/10.1007/s12043-019-1805-4

[20] Ali, Farhad, Anees Imtiaz, Ilyas Khan, and Nadeem Ahmad Sheikh. "Flow of magnetic particles in blood with isothermal heating: A fractional model for two-phase flow." *Journal of Magnetism and Magnetic Materials* 456 (2018): 413-422. https://doi.org/10.1016/j.jmmm.2018.02.063

[21] Ali, Farhad, Salman Yousaf, Ilyas Khan, and Nadeem Ahmad Sheikh. "A new idea of Atangana-Baleanu time fractional derivatives to blood flow with magnetics particles in a circular cylinder: two phase flow model." *Journal of Magnetism and Magnetic Materials* 486 (2019): 165282. https://doi.org/10.1016/j.jmmm.2019.165282

[22] Ali, Farhad, Anees Imtiaz, Ilyas Khan, Nadeem Ahmad Sheikh, and Dennis Ling Chuan Ching. "Hemodynamic flow in a vertical cylinder with heat transfer: two-phase Caputo Fabrizio fractional model." *Journal of Magnetics* 23, no. 2 (2018): 179-191. https://doi.org/10.4283/JMAG.2018.23.2.179

[23] Shah, Nehad Ali, Dumitru Vieru, and Constantin Fetecau. "Effects of the fractional order and magnetic field on the blood flow in cylindrical domains." *Journal of Magnetism and Magnetic Materials* 409 (2016): 10-19. https://doi.org/10.1016/j.jmmm.2016.02.013

[24] Saqib, Muhammad, Ilyas Khan, and Sharidan Shafie. "Generalized magnetic blood flow in a cylindrical tube with magnetite dusty particles." *Journal of Magnetism and Magnetic Materials* 484 (2019): 490-496. https://doi.org/10.1016/j.jmmm.2019.03.032

[25] Tabi, Conrad Bertrand, Pavel AY Ndjawa, Teko Ganakgomo Motsumi, C. D. K. Bansi, and Timoléon Crepin Kofané. "Magnetic field effect on a fractionalized blood flow model in the presence of magnetic particles and thermal radiations." *Chaos, Solitons & Fractals* 131 (2020): 109540. https://doi.org/10.1016/j.chaos.2019.109540

[26] Khan, Arshad, Dolat Khan, Ilyas Khan, Farhad Ali, and Muhammad Imran. "MHD flow of sodium alginate-based Casson type nanofluid passing through a porous medium with Newtonian heating." *Scientific reports* 8, no. 1 (2018): 1-12. https://doi.org/10.1038/s41598-018-26994-1

[27] Khaled, A-RA, and Kambiz Vafai. "The role of porous media in modeling flow and heat transfer in biological tissues." *International Journal of Heat and Mass Transfer* 46, no. 26 (2003): 4989-5003. https://doi.org/10.1016/S0017-9310(03)00301-6

[28] Kataria, Hari R., and Harshad R. Patel. "Soret and heat generation effects on MHD Casson fluid flow past an oscillating vertical plate embedded through porous medium." *Alexandria Engineering Journal* 55, no. 3 (2016): 2125-2137. https://doi.org/10.1016/j.aej.2016.06.024

[29] Kataria, HariR, and HarshadR Patel. "Heat and mass transfer in magnetohydrodynamic (MHD) Casson fluid flow past over an oscillating vertical plate embedded in porous medium with ramped wall temperature." *Propulsion and Power Research* 7, no. 3 (2018): 257-267. https://doi.org/10.1016/j.jppr.2018.07.003

[30] Kataria, Hari R., and Harshad R. Patel. "Effects of chemical reaction and heat generation/absorption on magnetohydrodynamic (MHD) Casson fluid flow over an exponentially accelerated vertical plate embedded in porous medium with ramped wall temperature and ramped surface concentration." *Propulsion and Power Research* 8, no. 1 (2019): 35-46. https://doi.org/10.1016/j.jppr.2018.12.001

[31] Iftikhar, Nazish, Dumitru Baleanu, Muhammad Bilal Riaz, and Syed Muhammad Husnine. "Heat and Mass Transfer of Natural Convective Flow with Slanted Magnetic Field via Fractional Operators." *Journal of Applied and Computational Mechanics* (2020).

[32] Rathod, V. P., and Shakera Tanveer. "Pulsatile flow of couple stress fluid through a porous medium with periodic body acceleration and magnetic field." *Bulletin of the Malaysian Mathematical Sciences Society* 32, no. 2 (2009).

[33] Paul, Ashish. "Magnetohydrodynamic unsteady natural convective flow in a porous medium over a moving infinite cylinder." *Heat Transfer* 51, no. 7 (2022): 6548-6562. https://doi.org/10.1002/htj.22612

[34] Bansi, C. D. K., C. B. Tabi, T. G. Motsumi, and A. Mohamadou. "Fractional blood flow in oscillatory arteries with thermal radiation and magnetic field effects." *Journal of Magnetism and Magnetic Materials* 456 (2018): 38-45. https://doi.org/10.1016/j.jmmm.2018.01.079

[35] Abro, Kashif Ali, and Abdon Atangana. "Porous effects on the fractional modeling of magnetohydrodynamic pulsatile flow: an analytic study via strong kernels." *Journal of Thermal Analysis and Calorimetry* 146, no. 2 (2021): 689-698. https://doi.org/10.1007/s10973-020-10027-z

[36] Maiti, Subrata, Sachin Shaw, and G. C. Shit. "Fractional order model for thermochemical flow of blood with Dufour and Soret effects under magnetic and vibration environment." *Colloids and Surfaces B: Biointerfaces* 197 (2021): 111395.

https://doi.org/10.1016/j.colsurfb.2020.111395

[37] Maiti, S., S. Shaw, and G. C. Shit. "Caputo–Fabrizio fractional order model on MHD blood flow with heat and mass transfer through a porous vessel in the presence of thermal radiation." *Physica A: Statistical Mechanics and its Applications* 540 (2020): 123149. https://doi.org/10.1016/j.physa.2019.123149

[38] Rao, I. J., and K. R. Rajagopal. "The effect of the slip boundary condition on the flow of fluids in a channel." *Acta Mechanica* 135, no. 3 (1999): 113-126. https://doi.org/10.1007/BF01305747

[39] Nubar, Yves. "Blood flow, slip, and viscometry." *Biophysical Journal* 11, no. 3 (1971): 252-264. https://doi.org/10.1016/S0006-3495(71)86212-4

[40] Ahmed, Sarfraz, and G C Hazarika, "Casson fluid Model for Blood flow with Velocity Slip in presence of Magnetic effect," *International Journal of Sciences: Basic and Applied Research (IJSBAR*, 5, no. 1, (2012): 1–8.

[41] Murthy, M. Krishna, Chakravarthula SK Raju, V. Nagendramma, Sabir Ali Shehzad, and Ali Jawad Chamkha. "Magnetohydrodynamics boundary layer slip Casson fluid flow over a dissipated stretched cylinder." In *Defect and Diffusion Forum*, vol. 393, pp. 73-82. Trans Tech Publications Ltd, 2019. https://doi.org/10.4028/www.scientific.net/DDF.393.73

[42] Ullah, Imran, Tawfeeq Abdullah Alkanhal, Sharidan Shafie, Kottakkaran Sooppy Nisar, Ilyas Khan, and Oluwole Daniel Makinde. "MHD slip flow of Casson fluid along a nonlinear permeable stretching cylinder saturated in a porous medium with chemical reaction, viscous dissipation, and heat generation/absorption." *Symmetry* 11, no. 4 (2019): 531. https://doi.org/10.3390/sym11040531

[43] Jalil, M., and W. Iqbal. "Numerical analysis of suction and blowing effect on boundary layer slip flow of Casson fluid along with permeable exponentially stretching cylinder." *AIP Advances* 11, no. 3 (2021). https://doi.org/10.1063/5.0042314

[44] Hayat, Tasawar, Muhammad Farooq, and A. Alsaedi. "Thermally stratified stagnation point flow of Casson fluid with slip conditions." *International Journal of Numerical Methods for Heat & Fluid Flow* 25, no. 4 (2015): 724-748. https://doi.org/10.1108/HFF-05-2014-0145

[45] Rogers, Kara, "Blood Vessel," *Encyclopedia Britannica*, 2023. [Online]. https://www.britannica.com/science/blood-vessel.

[46] Padma, R., R. Ponalagusamy, and R. Tamil Selvi. "Mathematical modeling of electro hydrodynamic non-Newtonian fluid flow through tapered arterial stenosis with periodic body acceleration and applied magnetic field." *Applied Mathematics and Computation* 362 (2019): 124453. https://doi.org/10.1016/j.amc.2019.05.024

[47] Jamil, Dzuliana Fatin, Salman Saleem, Rozaini Roslan, Fahad S. Al-Mubaddel, Mohammad Rahimi-Gorji, Alibek Issakhov, and Salah Ud Din. "Analysis of non-Newtonian magnetic Casson blood flow in an inclined stenosed artery using Caputo-Fabrizio fractional derivatives." *Computer Methods and Programs in Biomedicine* 203 (2021): 106044. https://doi.org/10.1016/j.cmpb.2021.106044

[48] Esfe, Mohammad Hemmat, Mehdi Bahiraei, Amirhesam Torabi, and Majid Valadkhani. "A critical review on pulsating flow in conventional fluids and nanofluids: Thermo-hydraulic characteristics." *International Communications in Heat and Mass Transfer* 120 (2021): 104859. https://doi.org/10.1016/j.icheatmasstransfer.2020.104859